Use of α_v Integrin Linked to Green Fluorescent Protein in Osteosarcoma Cells and Confocal Microscopy to Image Molecular Dynamics During Lung Metastasis in Nude Mice

YASUNORI TOME[1,2,3], SHUYA YANO[1,2], NAOTOSHI SUGIMOTO[4], SUMIYUKI MII[1,2], FUMINARI UEHARA[1,2,3], SHINJI MIWA[1,2,5], MICHAEL BOUVET[2], HIROYUKI TSUCHIYA[5], FUMINORI KANAYA[3] and ROBERT M. HOFFMAN[1,2]

[1]AntiCancer, Inc., San Diego, CA, U.S.A.;
[2]Department of Surgery, University of California, San Diego, CA, U.S.A.;
[3]Department of Orthopedic Surgery, Graduate School of Medicine, University of the Ryukyus, Nishihara, Japan;
Departments of [4]Physiology, and [5]Orthopaedic Surgery, Graduate School of Medical Science, Kanazawa University, Kanazawa, Ishikawa, Japan

Abstract. *Background: We report here imaging of the behavior of α_v integrin linked to green fluorescent protein (GFP) in human osteosarcoma cells colonizing the lung of nude mice. Materials and Methods: 143B osteosarcoma cells expressing α_v integrin–GFP were generated by transfection of an α_v integrin–GFP fusion-gene vector pCMV–AC– ITGAV–GFP. In order to generate experimental lung metastases, 143B osteosarcoma cells (1×10^6), stably expressing α_v integrin–GFP, were injected intravenously via the tail vein. The osteosarcoma cells were transplanted orthotopically in the tibia of nude mice in order to generate spontaneous metastases. Lungs were harvested and imaged by confocal microscopy within 1 hour. Results: In the experimental lung-metastasis model, extravasating and deformed osteosarcoma cells expressing α_v integrin–GFP were observed. Pseudopodia of the osteosarcoma cells contained small puncta of α_v integrin–GFP. In early-stage spontaneous lung metastasis, tumor emboli were observed in pulmonary vessels. At high magnification, small α_v integrin–GFP puncta were observed in the tumor embolus. In late-stage spontaneous metastasis, tumor emboli were also observed in pulmonary vessels. Invading cancer cells with strong expression of α_v integrin–GFP were observed at the margin of the tumor emboli. Conclusion: The results of this study demonstrate that molecular dynamics of α_v integrin–GFP can be imaged in lung metastasis, which will allow further understanding of the role of α_v integrin in this process. The results also suggest a general concept for imaging molecular behavior in vivo.*

This article is freely accessible online.

Correspondence to: Robert M. Hoffman, Ph.D., AntiCancer, Inc., 7917 Ostrow Street, San Diego, CA 92111, U.S.A. Tel: +1 8586542555, Fax: +1 8582684175, e-mail: all@anticancer.com

Key Words: α_v Integrin, green fluorescent protein, osteosarcoma, real-time imaging, confocal microscopy, nude mice, lung metastasis.

The α_v integrin subfamily consists of at least five members including $\alpha_v\beta_1$, $\alpha_v\beta_3$, $\alpha_v\beta_5$, $\alpha_v\beta_6$, and $\alpha_v\beta_8$ (1) and have been implicated in tumor progression (2-5), including osteosarcoma (6). In a previous study, we used a powerful subcellular *in vivo* imaging model to demonstrate how an anti-integrin antibody inhibits seeding to and growth of osteosarcoma cells on the lung (7). The 143B human osteosarcoma cell line, expressing red fluorescent protein (RFP) in the cytoplasm and green fluorescent protein (GFP) in the nucleus, was established. Such double-labeled cells enable imaging of apoptosis and mitosis and other nuclear–cytoplasmic dynamics. Using these double-labeled osteosarcoma cells, single cancer-cell seeding in the lung after *i.v.* injection of osteosarcoma cells was imaged in real time (7). The anti-β1 integrin monoclonal antibody, AIIB2, greatly inhibited the seeding of cancer cells on the lung (experimental metastasis), while a control antibody had no effect. AIIB2 also significantly inhibited spontaneous lung metastasis from 143B-GFP-RFP tumors growing in the tibia but not primary tumor growth, possibly due to inhibition of lung seeding of the cancer cells, as imaged in the experimental metastasis study. AIIB2 treatment also increased survival of mice with orthotopically growing 143B-RFP (7).

We then began to develop imaging of molecular dynamics *in vivo*. For this purpose, we used 143B osteosarcoma cells

expressing an α_v integrin–GFP fusion gene in order to visualize the molecular dynamics of α_v integrin in osteosarcoma cells interacting with RFP-expressing blood vessels using color-coded imaging (8).

We previously developed subcellular *in vivo* imaging (9-34). In the present report, we demonstrate subcellular imaging of α_v integrin behavior in osteosarcoma cells during lung metastasis. In this study, we imaged the molecular dynamics of α_v integrin–GFP in osteosarcoma cells (34) during experimental and spontaneous lung metastasis in nude mice.

Materials and Methods

Cells. The 143B human osteosarcoma cell line was maintained with RPMI-1640 medium (Irvine Scientific, Santa Ana, CA, USA) containing 10% fetal bovine serum (FBS) (Omega Scientific, San Diego, CA, USA) and 1% penicillin/streptomycin at 37˚C in a humidified incubator with 5% CO_2.

Establishment of human osteosarcoma cells expressing α_v integrin–GFP. The pCMV6-AC-ITGAV-GFP vector, containing α_v integrin linked to GFP, was obtained from OriGene Technologies (Rockville, MD, USA). 143B cells were transformed to express α_v integrin–GFP as follows: At 80% confluency, cultures were transfected with pCMV-AC-ITGAV-GFP using Lipofectamine LTX (Invitrogen, Carlsbad, CA, USA) according to the manufacturer's instruction. After transfection, stable cells were selected with G418 (800 μg/ml) (Sigma-Aldrich, St. Louis, MO, USA), starting at 24 h after transfection. Stable colonies were selected and maintained in RPMI-1640 medium containing 10% FBS and 500 μg/ml G418 (8, 35).

Experimental and spontaneous lung metastasis models in nude mice. Nude (nu/nu) mice were bred and housed in a barrier facility (AntiCancer Inc., San Diego, CA, USA). To image experimental lung metastases of nude mice, 143B cells (1×10^6) expressing α_v integrin–GFP were injected into the tail vein of 4- to 5-week-old nude mice. Twenty-four hours after injection, nude mice were euthanized with a ketamine mixture (10 μl ketamine HCl, 7.6 μl xylazine, 2.4 μl acepromazine maleate, and 10 μl water) (Butler-Schein, Dublin, OH, USA). Lungs were harvested from each mouse at necropsy and were placed on a glass slide with a cover. To image spontaneous lung metastases in nude mice, 143B cells (1×10^6) expressing α_v integrin–GFP, were transplanted into the left tibia of 4- to 5-week-old nude mice as previously described (36). Mice were euthanized 4 and 8 weeks after implantation, and lungs were harvested and observed. All animal studies were conducted in accordance with the principals and procedures outlined in the NIH Guide for the Care and Use of Laboratory Animals under assurance number A3873-1.

Imaging. Imaging was performed with an FV 1000 laser-scanning confocal microscope (Olympus, Tokyo, Japan) with a XLUMPLFL 20× (0.95 NA) water-immersion objective (37). GFP was excited at 488 nm. Collagen fibers were imaged in reflectance mode with excitation at 488 nm, and scattered (reflected) photons were collected at the same wavelength. Images were produced with FV10-ASW Fluoview software (Olympus) and ImageJ (NIH, Bethesda, MD, USA) and were not modified beyond the standard adjustment of intensity levels.

Results and Discussion

143B cells expressing α_v integrin–GFP. 143B α_v integrin–GFP cells have strikingly bright GFP fluorescence in the cytoplasm *in vitro* (Figure 1A). Fibronectin is an extracellular ligand binding to α_v integrin (37). When 143B α_v integrin–GFP cells were seeded on a fibronectin-coated dish (BD Pharmingen, San Diego, CA, USA), punctate expression of α_v integrin–GFP was observed interacting with fibronectin coated on the culture dish (Figure 1B).

Imaging 143B α_v integrin–GFP experimental lung metastases in nude mice. To understand the molecular dynamics of α_v integrin–GFP in osteosarcoma experimental lung metastasis, 143B α_v integrin–GFP cells were injected into the tail vein of nude mice. Twenty-four hours after injection, lungs were harvested and observed by confocal microscopy. A single cancer cell with small α_v integrin–GFP puncta was observed on the surface of the lung (Figure 2A). Extravasating and deformed osteosarcoma cells expressing α_v integrin–GFP were also observed (Figure 2B). There were multiple pseudopodia of osteosarcoma cells with small α_v integrin–GFP puncta (Figure 2C). These results suggested that the behavior of α_v integrin is associated with cancer-cell adaptation to the pulmonary microenvironment at an early stage of lung metastasis.

Imaging of early-stage 143B α_v integrin–GFP spontaneous lung metastases. In order to image the molecular dynamics of α_v integrin–GFP in osteosarcoma cells during spontaneous lung metastasis, we transplanted osteosarcoma cells into the tibia of nude mice to generate a primary bone tumor, which subsequently spontaneously generated lung metastases. Four weeks after implantation, lungs were harvested and observed. Tumor emboli were observed in pulmonary vessels. The expression of α_v integrin–GFP was scattered in the emboli (Figure 3A). With higher magnification, small α_v integrin–GFP puncta were also observed in the tumor embolus (Figure 3B). Osteosarcoma cells adjacent to lung tissue had puncta strongly expressing α_v integrin–GFP (Figure 3C). Metastatic cells around a small vessel, strongly expressed diffuse α_v integrin–GFP (Figure 3D).

Imaging of late-stage spontaneous lung metastases of 143B α_v integrin–GFP cells. In order to image the behavior of α_v integrin–GFP in osteosarcoma cells in late-stage spontaneous lung metastases, lungs were harvested 8 weeks after orthotopic implantation of 143B cells into the tibia and examined. Tumor emboli were observed in pulmonary vessels (Figure 4A). Invading cancer cells with strong expression of α_v integrin–GFP were observed at the margin of tumor emboli (Figure 4A). Spontaneously invading

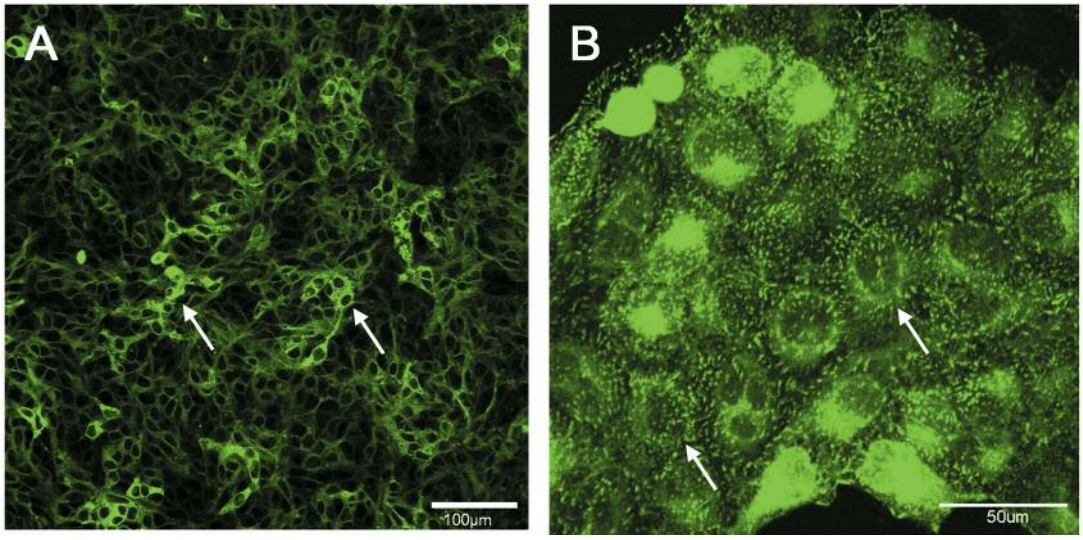

Figure 1. *143B cells expressing α_v integrin–green fluorescent protein (GFP). A: 143B cells stably expressing α_v integrin–GFP in vitro. Bar: 100 μm. B: Punctate expression of α_v integrin–GFP was observed at the bottom of the cells binding to fibronectin coated on the plastic cell-culture dish. Bar: 50 μm. FV1000 confocal microscopy.*

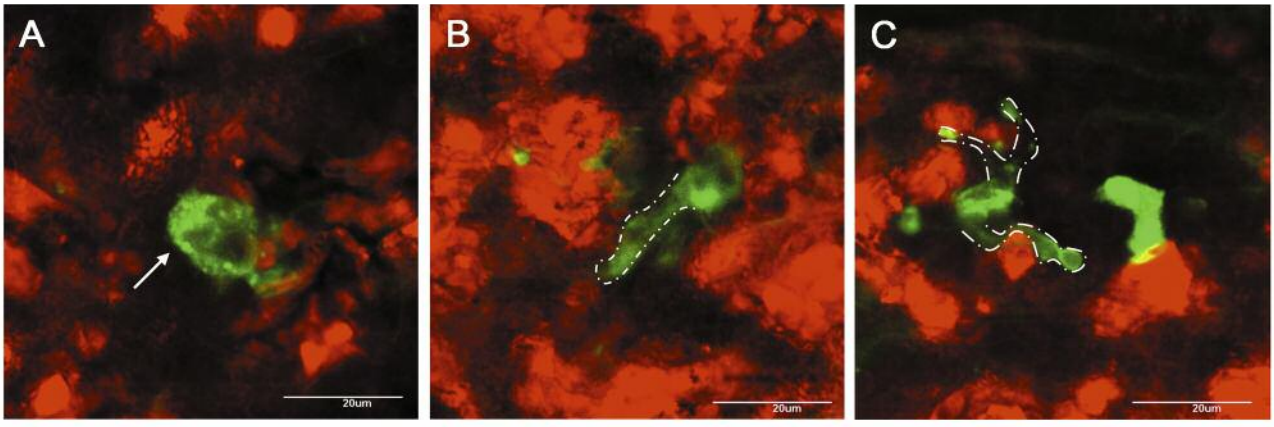

Figure 2. *Imaging of α_v integrin–green fluorescent protein (GFP) molecular dynamics in experimental lung metastases of 143B osteosarcoma cells in nude mice. A: Small α_v integrin–GFP puncta in the cytoplasm of a 143B cell. B: Extravasating deformed 143B cells have α_v integrin–GFP puncta. C: Multiple pseudopodia of 143B cells with small α_v integrin–GFP puncta. Bar: 20 μm. FV1000 confocal microscopy.*

osteosarcoma cells had extensive α_v integrin–GFP puncta (Figure 4B). With higher magnification, α_v integrin–GFP puncta were readily imaged at the subcellular level (Figure 4C) and pseudopodia with small α_v integrin puncta were observed (Figure 4D).

The *in vivo* molecular imaging technology and mouse models of osteosarcoma metastasis described in the present report will be a very valuable tool for investigating the molecular dynamics of α_v integrin and other proteins in lung metastasis of osteosarcoma (7, 19, 38). The results also suggest a general concept for imaging molecular behavior *in vivo*.

Conflicts of Interest

No potential conflicts of interest were disclosed.

Dedication

This paper is dedicated to the memory of A. R. Moossa, M.D., and Sun Lee, M.D.

References

1 Hynes RO: Integrins: Bidirectional, allosteric signaling machines. Cell *110*: 673-687, 2002.

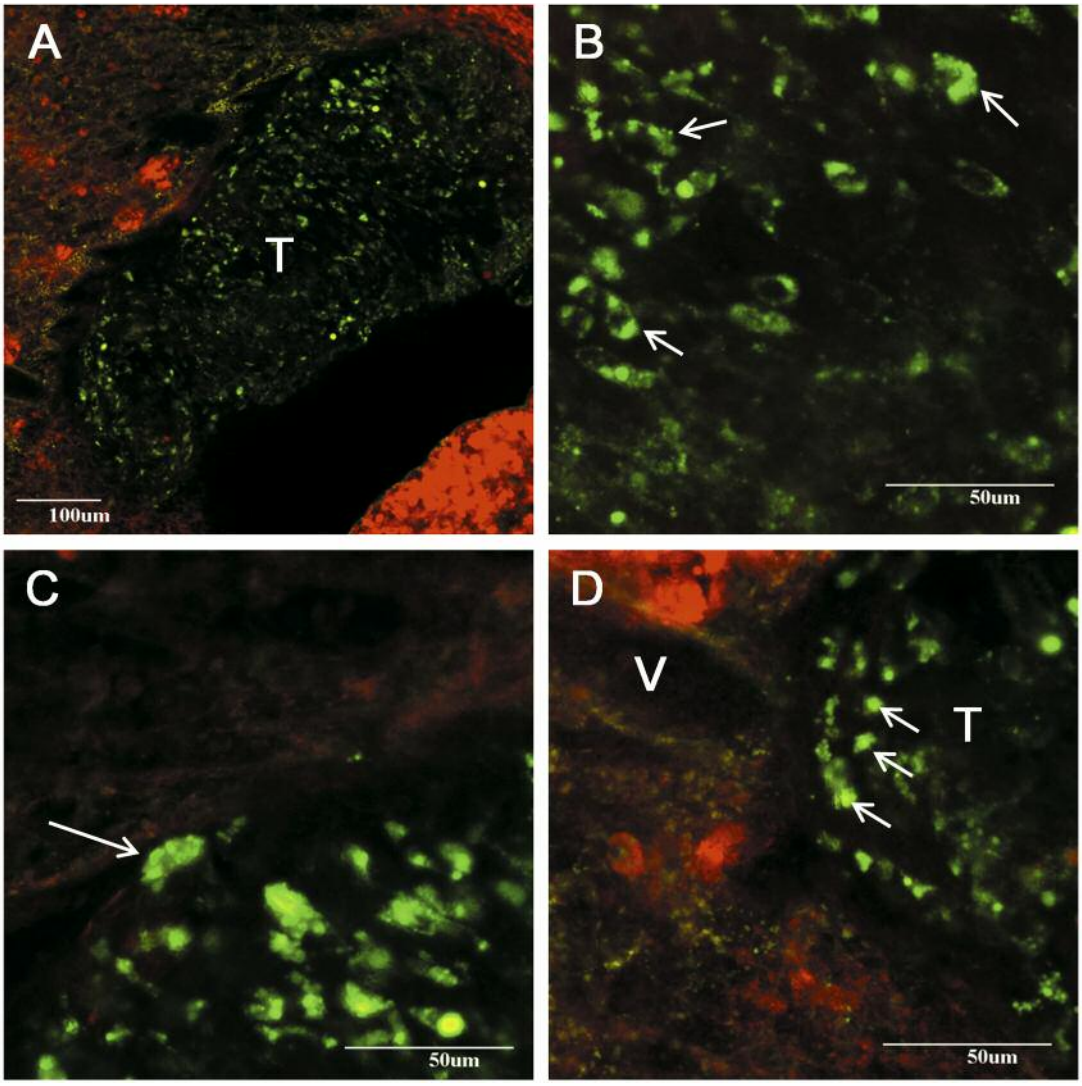

Figure 3. *Imaging of α_v integrin–green fluorescent protein (GFP) molecular dynamics in 143B spontaneous lung metastases in nude mice (early stage). A: Tumor embolus in a large vessel in the lung. Diffuse expression of α_v integrin–GFP in the 143B osteosarcoma cells in the tumor embolus. Bar: 100 μm. B: Small α_v integrin–GFP puncta observed at higher magnification (×40). Bar: 50 μm. C: Osteosarcoma cells adjacent to lung tissue with puncta strongly expressing α_v integrin–GFP (arrow). Bar: 50 μm. D: Cells strongly expressing α_v integrin–GFP surrounded a smaller vessel (V). Bar: 50 μm. FV1000 confocal microscopy. T: Tumor. V: Vessel.*

2 Stupack DG and Cheresh DA: Integrins and angiogenesis. Curr Top Dev Biol *64*: 207-238, 2004.

3 Marshall JF and Hart IR: The role of αv-integrins in tumour progression and metastasis. Semin Cancer Biol *7*: 129-138, 1996.

4 Tucker GC: α_v integrin inhibitors and cancer therapy. Curr Opin Investig Drugs *4*: 722-731, 2003.

5 Hood JD and Cheresh DA: Role of integrins in cell invasion and migration. Nat Rev Cancer *2*: 91-100, 2002.

6 Duan X, Jia SF, Zhou Z, Langley RR, Bolontrade MF and Kleinerman ES: Association of αvβ3 integrin expression with the metastatic potential and migratory and chemotactic ability of human osteosarcoma cells. Clin Exp Metastatsis *21*: 747-753, 2004.

7 Kimura H, Tome Y, Momiyama M, Hayashi K, Tsuchiya H, Bouvet M and Hoffman RM: Imaging the inhibition by anti-β1 integrin antibody of lung seeding of single osteosarcoma cells in live mice. Int J Cancer *131*: 2027-2033, 2012.

8 Uehara F, Tome Y, Yano S, Miwa S, Mii S, Hiroshima Y, Bouvet M, Maehara H, Kanaya F and Hoffman RM: A color-coded imaging model of the interaction of α_v integrin–GFP expressed in osteosarcoma cells and RFP expressing blood vessels in Gelfoam® vascularized *in vivo*. Anticancer Res *33*: 1361-1366, 2013.

9 Yamamoto N, Jiang P, Yang M, Xu M, Yamauchi K, Tsuchiya H, Tomita K, Wahl GM, Moossa AR and Hoffman RM: Cellular dynamics visualized in live cells *in vitro* and *in vivo* by differential dual-color nuclear–cytoplasmic fluorescent-protein expression. Cancer Res *64*: 4251-4256, 2004.

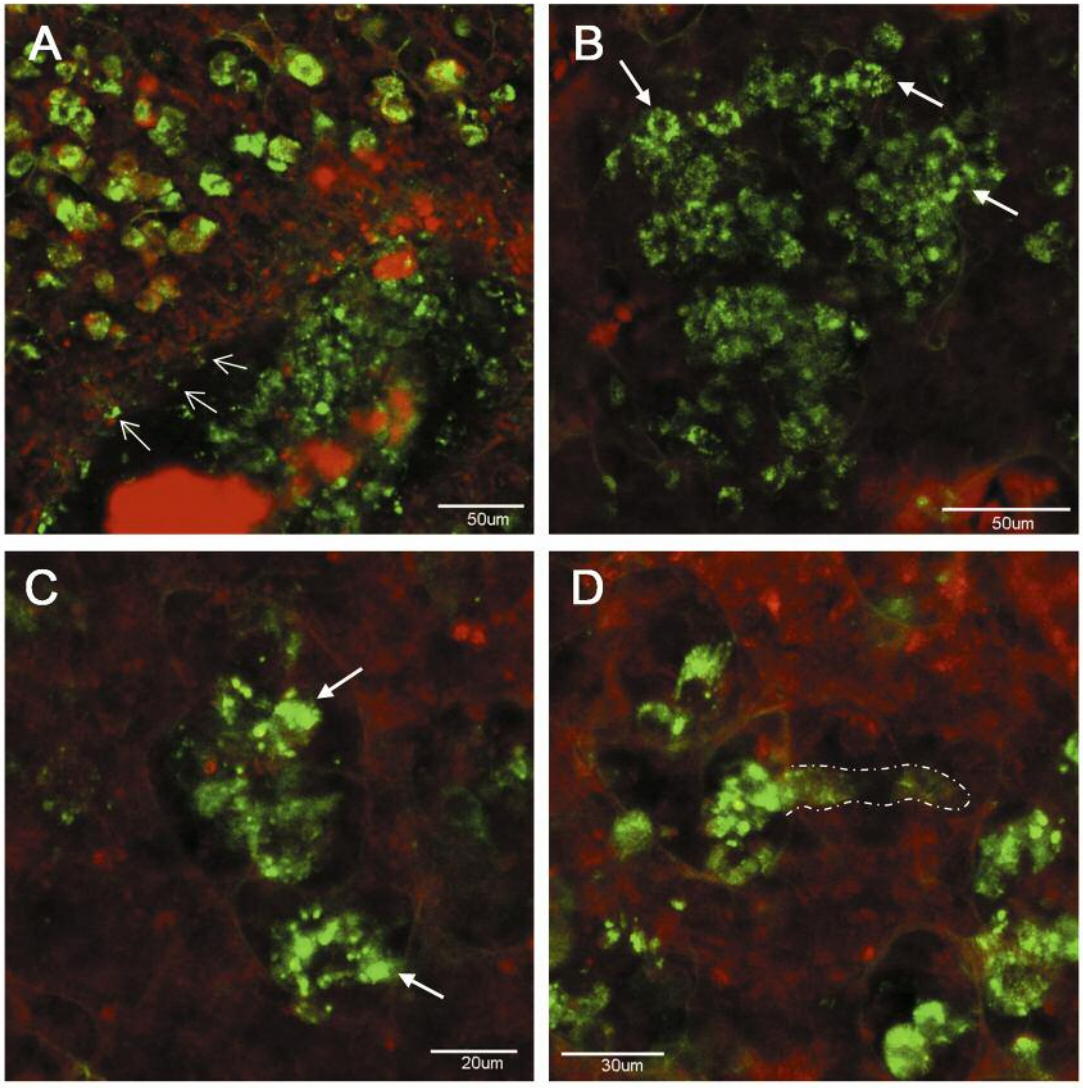

Figure 4. *Imaging of α_v integrin–green fluorescent protein (GFP) molecular dynamics in spontaneous lung metastases of 143B cells in nude mice (late stage). A: Tumor embolus in pulmonary vessel. Invading cancer cells with strong expression of α_v integrin–GFP at the margin of the embolus (arrows). Bar: 50 μm. B: Invading cancer cells with more α_v integrin–GFP puncta. Bar: 50 μm. C: α_v integrin–GFP puncta higher magnification (×60). Bar: 20 μm. D: Pseudopodium of 143B cells with small α_v integrin–GFP puncta. Bar: 30 μm. FV1000 confocal microscopy.*

10 Zhao M, Yang M, Li X-M, Jiang P, Baranov E, Li S, Xu M, Penman S and Hoffman RM: Tumor-targeting bacterial therapy with amino acid auxotrophs of GFP-expressing *Salmonella typhimurium*. Proc Natl Acad Sci USA *102*: 755-760, 2005.

11 Yamauchi K, Yang M, Jiang P, Yamamoto N, Xu M, Amoh Y, Tsuji K, Bouvet M, Tsuchiya H, Tomita K, Moossa AR and Hoffman RM: Real-time *in vivo* dual-color imaging of intracapillary cancer cell and nucleus deformation and migration. Cancer Res *65*: 4246-4252, 2005.

12 Tsuji K, Yamauchi K, Yang M, Jiang P, Bouvet M, Endo H, Kanai Y, Yamashita K, Moossa AR and Hoffman RM: Dual-color imaging of nuclear–cytoplasmic dynamics, viability, and proliferation of cancer cells in the portal vein area. Cancer Res *66*: 303-306, 2006.

13 Yamauchi K, Yang M, Jiang P, Xu M, Yamamoto N, Tsuchiya H, Tomita K, Moossa AR, Bouvet M and Hoffman RM: Development of real-time subcellular dynamic multicolor imaging of cancer cell-trafficking in live mice with a variable-magnification whole-mouse imaging system. Cancer Res *66*: 4208-4214, 2006.

14 Jiang P, Yamauchi K, Yang M, Tsuji K, Xu M, Maitra A, Bouvet M and Hoffman RM: Tumor cells genetically labeled with GFP in the nucleus and RFP in the cytoplasm for imaging cellular dynamics. Cell Cycle *5*: 1198-1201, 2006.

15 Hoffman RM and Yang M: Subcellular imaging in the live mouse. Nature Protocols *1*: 775-782, 2006.

16 Yang M, Jiang P and Hoffman RM: Whole-body subcellular multicolor imaging of tumor-host interaction and drug response in real time. Cancer Res *67*: 5195-5200, 2007.

17 Hu M, Zhao M, An C, Yang M, Li Q, Zhang Y, Suetsugu A, Tome Y, Yano S, Fu Y, Hoffman RM and Hu K: Real-time imaging of apoptosis induction of human breast cancer cells by the traditional Chinese medicinal herb tubeimu. Anticancer Res *32*: 2509-2514, 2012.

18 Hiroshima Y, Maawy A, Hassanein MK, Menen R, Momiyama M, Murakami T, Miwa S, Yamamoto M, Uehara F, Yano S, Mori R, Matsuyama R, Chishima T, Tanaka K, Ichikawa Y, Bouvet M, Endo I and Hoffman RM: The tumor-educated macrophage increase of malignancy of human pancreatic cancer is prevented by zoledronic acid. PLoS One *9*: e103382, 2014.

19 Kimura H, Hayashi K, Yamauchi K, Yamamoto N, Tsuchiya H, Tomita K, Kishimoto H, Bouvet M and Hoffman RM: Real-time imaging of single cancer-cell dynamics of lung metastasis. J Cell Biochem *109*: 58-64, 2010.

20 Kimura H, Lee C, Hayashi K, Yamauchi K, Yamamoto N, Tsuchiya H, Tomita K, Bouvet M and Hoffman RM: UV light killing efficacy of fluorescent protein-expressing cancer cells *in vitro* and *in vivo*. J Cell Biochem *110*: 1439-1446, 2010.

21 Hayashi K, Kimura H, Yamauchi K, Yamamoto N, Tsuchiya H, Tomita K, Kishimoto H, Hasegawa A, Bouvet M and Hoffman RM: Comparison of cancer-cell seeding, viability and deformation in the lung, muscle and liver, visualized by subcellular real-time imaging in the live mouse. Anticancer Res *31*: 3665-3672, 2011.

22 Yamauchi K, Tome Y, Yamamoto N, Hayashi K, Kimura H, Tsuchiya H, Tomita K, Bouvet M and Hoffman RM: Color-coded real-time subcellular fluorescence imaging of the interaction between cancer and host cells in live mice. Anticancer Res *32*: 39-43, 2012.

23 Amoh Y, Hamada Y, Katsuoka K and Hoffman RM: *In vivo* imaging of nuclear-cytoplasmic deformation and partition during cancer cell death due to immune rejection. J Cell Biochem *113*: 465-472, 2012.

24 Zhang L, Wu C, Zhang Y, Liu F, Wang X, Zhao M and Hoffman RM: Comparison of efficacy and toxicity of Traditional Chinese Medicine (TCM) herbal mixture LQ and conventional chemotherapy on lung cancer metastasis and survival in mouse models. PLoS One *9*: e109814, 2014.

25 Suetsugu A, Hassanein MK, Reynoso J, Osawa Y, Nagaki M, Moriwaki H, Saji S, Bouvet M and Hoffman RM: The cyan fluorescent protein nude mouse as a host for multicolor-coded imaging models of primary and metastatic tumor microenvironments. Anticancer Res *32*: 31-38, 2012.

26 Momiyama M, Suetsugu A, Kimura H, Kishimoto H, Aki R, Yamada A, Sakurada H, Chishima T, Bouvet M, Bulgakova NN, Endo I and Hoffman RM: Fluorescent proteins enhance UVC PDT of cancer cells. Anticancer Res *32*: 4327-4330, 2012.

27 Momiyama M, Suetsugu A, Chishima T, Bouvet M, Endo I, and Hoffman RM: Subcellular real-time imaging of the efficacy of temozolomide on cancer cells in the brain of live mice. Anticancer Res *33*: 103-106, 2013.

28 Momiyama M, Suetsugu A, Kimura H, Kishimoto H, Aki R, Yamada A, Sakurada H, Chishima T, Bouvet M, Endo I and Hoffman RM: Imaging the efficacy of UVC irradiation on superficial brain tumors and metastasis in live mice at the subcellular level. J Cell Biochem *114*: 428-434, 2013.

29 Momiyama M, Suetsugu A, Kimura H, Chishima T, Bouvet M, Endo I and Hoffman RM: Dynamic subcellular imaging of cancer cell mitosis in the brain of live mice. Anticancer Res *33*: 1367-1371, 2013.

30 Tome Y, Kimura H, Maehara H, Sugimoto N, Bouvet M, Tsuchiya H, Kanaya F, Hoffman RM: High lung-metastatic variant of human osteosarcoma cells, selected by passage of lung metastasis in nude mice, is associated with increased expression of αvβ3 integrin. Anticancer Res *33*: 3623-3628, 2013.

31 Suetsugu A, Jiang P, Moriwaki H, Saji S, Bouvet M and Hoffman RM: Imaging nuclear–cytoplasm dynamics of cancer cells in the intravascular niche of live mice. Anticancer Res *33*: 4229-4236, 2013.

32 Suetsugu A, Jiang P, Yang M, Yamamoto N, Moriwaki H, Saji S and Hoffman RM: The use of living cancer cells expressing green fluorescent protein in the nucleus and red fluorescence protein in the cytoplasm for real-time confocal imaging of chromosome and cytoplasmic dynamics during mitosis. Anticancer Res *35*: 2545-2551, 2015.

33 Yang M, Jiang P and Hoffman RM: Early reporting of apoptosis by real-time imaging of cancer cells labeled with green fluorescent protein in the nucleus and red fluorescent protein in the cytoplasm. Anticancer Res *35*: 2539-2543, 2015.

34 Hoffman RM ed.). *In Vivo* Cellular Imaging Using Fluorescent Proteins: Methods and Protocols. Methods in Molecular Biology, Vol. 872. Walker, John M. (series ed.) Humana Press (Springer Science+Business Media), New York, 2012.

35 Tome Y, Sugimoto N, Yano S, Momiyama M, Mii S, Maehara H, Bouvet M, Tsuchiya H, Kanaya F and Hoffman RM: Real-time imaging of a_v integrin molecular dynamics in osteosarcoma cells *in vitro* and *in vivo*. Anticancer Res *33*: 3021-3025, 2013.

36 Tome Y, Tsuchiya H, Hayashi K, Yamauchi K, Sugimoto N, Kanaya F, Tomita K and Hoffman RM: *In vivo* gene transfer between interacting human osteosarcoma cell lines is associated with acquisition of enhanced metastatic potential. J Cell Biochem *108*: 362-370, 2009.

37 Uchugonova A, Duong J, Zhang N, König K and Hoffman RM: The bulge area is the origin of nestin-expressing pluripotent stem cells of the hair follicle. J Cell Biochem *112*: 2046-2050, 2011.

38 Marshall JF and Hart IR: The role of av-integrins in tumour progression and metastasis. Semin Cancer Biol *7*: 129-138, 1996.

39 Kreisel D, Nava RG, Li W, Zinselmeyer BH, Wang B, Lai J, Pless R, Gelman AE, Krupnick AS and Miller MJ: *In vivo* tow-photon imaging reveals monocyte-depedent neutrophil extravasation during pulmonary inflammation. Proc Natl Acad Sci USA *107*: 18073-18078, 2010.

Received May 2, 2016
Revised June 5, 2016
Accepted June 7, 2016